



Full paper/Mémoire

## Synthesis of silver tin oxide nanocomposite powders via chemical coprecipitation method

F. Shakerian, N. Parvin\*, A. Azadmehr, M.R. Rabiei

Department of mining and materials engineering, Amirkabir University of Technology, (Tehran Polytechnic), Tehran, 15875-4413, Iran

## ARTICLE INFO

## Article history:

Received 28 November 2011

Accepted after revision 7 May 2012

Available online 18 June 2012

## Keywords:

Nanocomposite

Silver tin oxide

Contact materials

Coprecipitation

Supersaturation

Ionic strength

Preliminary compounds

## ABSTRACT

A nanocomposite powder Ag-SnO<sub>2</sub> was produced by the chemical coprecipitation technique using Sn element, SnCl<sub>2</sub>·2H<sub>2</sub>O and silver nitrate as starting materials and carbonate solutions as precipitating agents. The effect of the chlorine ion, ionic strength and supersaturation were investigated for nanopowder using X-ray diffraction analysis (XRD), scanning electron microscopy (SEM) and X-ray mapping. The fine and uniformly dispersed microstructure are attained by using coprecipitation method. Higher ionic strength leads to lower particle size of nanocomposite. The undesirable chlorine ion, which leads to instability in contact surface, is eliminated by replacing SnCl<sub>2</sub>·2H<sub>2</sub>O instead of Sn element as starting material. Also the degree of agglomeration decreases with this change. The results show that the increasing in the supersaturation of environment enhances the nucleation. So it causes a reduction in the nanocomposite particle size to 50%.

© 2012 Published by Elsevier Masson SAS on behalf of Académie des sciences.

### 1. Introduction

Silver-metal oxide composite contact materials have a variety of applications in low voltage switches such as relays, contactors and circuit breakers [1–4]. Until three decades ago, Ag-CdO composite was the preferred material for these usages due to excellent functional and technological properties. However, because of toxic nature of Cd, especially when it is evaporated, considerable efforts have been made to replace it with environment-friendly substances such as Ag-SnO<sub>2</sub> [2–9]. Ag-SnO<sub>2</sub> materials, in addition, have higher hardness, contact resistance and temperature rise than Ag-CdO substances. Besides their arc erosion and anti-welding properties are excellent [10–12].

There are different methods such as powder metallurgy, casting and chemical methods for producing Ag-SnO<sub>2</sub> materials [13]. Recently, chemical coprecipitation has been widely used to synthesize complex powders, because of economically viable, homogenous distribution of particles and possibility of achieving nanosized powders [14]. In this paper, nanosized Ag-SnO<sub>2</sub> powders were synthesized by chemical coprecipitation technique. In order to obtain nanoparticles with a narrow size distribution, the following requirements should be met:

- high degree of supersaturation;
- uniform spatial concentration distribution inside a reactor;
- uniform growth time for all particles or crystals [15].

The ionic strength of tin and supersaturation of precipitant have direct effect on final properties. For discussing about influence of preliminary compounds, the ionic strength of tin and supersaturation of precipitant, two nitrate compounds of silver and tin were precipitated in carbonate agents simultaneously. Then they were calcinated at 400 °C for 4 hours.

\* Corresponding author.

E-mail addresses: f\_shakerian@aut.ac.ir (F. Shakerian), nparvin@aut.ac.ir (N. Parvin), a\_azadmehr@aut.ac.ir (A. Azadmehr), mreza.r@aut.ac.ir (M.R. Rabiei).

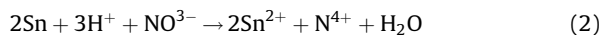
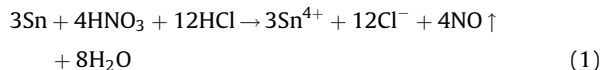
## 2. Materials and methods

The chemical coprecipitation method is considered to be a suitable method to prepare Ag-SnO<sub>2</sub> composite powders. Nitrates of silver and tin were precipitated in carbonate agents simultaneously. Then they were calcined at 400 °C for 4 hours. Phase structures of the as-prepared samples were examined by X-ray diffraction (XRD) with Cu K $\alpha$  radiation at an operation voltage and current 40 kV and 40 mA, respectively. The grain size was calculated by using the Debye-Scherrer's equation. The particle morphology, microstructure and particle size of nanopowders were observed by scanning Electron Microscopy (SEM) type Philips XL30. The distribution of particles was studied by X-ray mapping.

## 3. Experimental

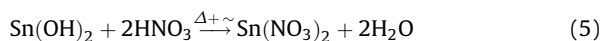
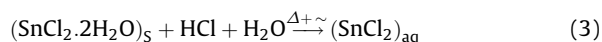
Two kinds of tin ion (Sn<sup>2+</sup> and Sn<sup>4+</sup>) with different ionic strengths exist. Ag-SnO<sub>2</sub> nanoparticles were synthesized with different preliminary compound and reaction agents as follows.

Firstly, DPT(II)<sup>1</sup> method: Tin powders were dissolved in warm and thin nitric acid while they were stirred. Since SnO<sub>2</sub> powders were formed so quickly, several drops of HCl solution were added to prevent the formation of SnO<sub>2</sub>, which can be expressed by the Eq. (1). If SnO<sub>2</sub> powders are formed at this stage, homogenous distribution of nano-sized SnO<sub>2</sub> particles in silver matrix is not achieved. Tin nitrate solution (II) was formed according to Eq. (2):



Secondly, DPT(IV)<sup>2</sup> method: tin nitrate solution (IV) was formed by adding 20 mL heavy nitric acid to tin nitrate solution (II) while it was warmed up to 55 °C.

Thirdly, DPC<sup>3</sup> method: SnCl<sub>2</sub>.2H<sub>2</sub>O powders were dissolved in deionised water and few drops of hydrochloric acid was added to ensure dissolution at the boiling temperature. Sn(OH)<sub>2</sub> precipitation was formed by adding NaOH solution. The resulting product was dissolved in nitric acid, after which the Sn(OH)<sub>2</sub> precipitate was washed with deionized water several times to remove chlorine ions. The resulting reactions can be described as follows:



Tin and silver nitrate solutions were dropped to the precipitating agents (Na<sub>2</sub>CO<sub>3</sub>, M = 1.9 m/L; NaHCO<sub>3</sub>, M = 1.3 m/L; K<sub>2</sub>CO<sub>3</sub>, M = 7.5 m/L) from two separated

<sup>1</sup> Direct processing Tin(II).

<sup>2</sup> Direct processing Tin(IV).

<sup>3</sup> Direct processing Tin Chlorine.

**Table 1**

Synthesis conditions of silver tin oxide nanocomposite powders.

Sample	Preliminary compound	Sn ion	Precipitant
DPT(II)	Sn(metal)	Sn <sup>2+</sup>	Na <sub>2</sub> CO <sub>3</sub> /M = 1.9
DPT(IV)	Sn(metal)	Sn <sup>4+</sup>	Na <sub>2</sub> CO <sub>3</sub> /M = 1.9
DPC-I	SnCl <sub>2</sub> · 2H <sub>2</sub> O	Sn <sup>2+</sup>	Na <sub>2</sub> CO <sub>3</sub> /M = 1.9
DPC-II	SnCl <sub>2</sub> · 2H <sub>2</sub> O	Sn <sup>2+</sup>	K <sub>2</sub> CO <sub>3</sub> /M = 7.5
DPC-III	SnCl <sub>2</sub> · 2H <sub>2</sub> O	Sn <sup>2+</sup>	NaHCO <sub>3</sub> /M = 1.3

DPT: direct processing tin; DPC: direct processing tin chlorine.

capsules slowly (0.05 cm<sup>3</sup>/sec). In all processes, the resulting powders were washed with deionised water for several times, dried at 100 °C for 2 hours and were calcined at 400 °C for 4 h. The synthesis conditions of Ag-SnO<sub>2</sub> nanopowders are listed in Table 1.

## 4. Result and discussion

### 4.1. The effect of ionic strength

The average crystallite size of the silver nanoparticles was calculated according to the Debye-Scherrer's equation as follows:

$$D = K\lambda / \beta \cos\theta_\beta \quad (6)$$

where  $D$  is the crystallite size,  $K$  is a grain shape factor (0.9),  $\lambda$  is the beam wavelength,  $\theta_\beta$  is the diffraction angle, and  $\beta$  is the full-width at half-maximum of the peak (FWHM). The grain size of silver particle is shown in Table 2. The width of the diffraction line at half its maximum intensity for silver element is narrower than that of tin oxide.

Fig. 1 shows the XRD pattern of DPT(II). Similar pattern was observed for PDT(IV). It can be seen that the final composition of two powders are equal since the preliminary compound is metal tin, the AgCl peaks are recognized.

The SEM micrographs of DPT(II) and DPT(IV) powders are shown in Fig. 2.

For solutions with ionic strengths of 0.1 M or less, the electrolyte effects is independent of the kind of ions and dependent only on the ionic strength. This independence with respect to electrolyte species disappears at high ionic strength.

According to the Eq. (7) (Debye-Huckel Equation), it is evident that Sn(II) has higher activity coefficient in the same ionic strength of Sn(II) and Sn(IV).

$$-\log\gamma_x = 0.51Z_x^2\sqrt{\mu} / (1 + 3.3\alpha_x\sqrt{\mu}) \quad (7)$$

where:

- $\gamma_x$  = activity coefficient of the species X;
- $Z_x$  = charge on the species X;

**Table 2**

Calculated grain size (110)<sub>Ag</sub>.

Sample	Grain size(nm)
DPT(II)	83.1
DPT(IV)	89.6
DPC-I	29.7
DPC-II	26.3
DPC-III	29.7

DPT: direct processing tin; DPC: direct processing tin chlorine.

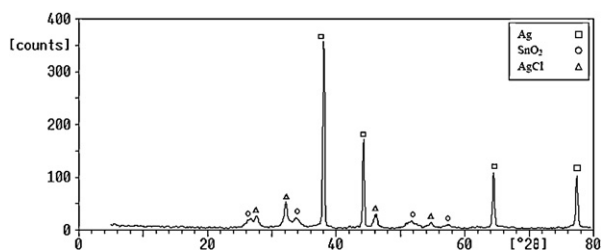


Fig. 1. X-ray diffraction (XRD) patterns of DPT(II) powder. DPT: direct processing tin.

- $\mu$  = ionic strength of the solution;
- $\alpha_x$  = effective diameter of the hydrated ion X in nanometers ( $10^{-9}$ m).

The larger the charge of an ion, the larger number of polar water molecules that will be held in the solution shell about the ion [16].

The effective diameter of the hydrated  $\text{Sn}^{+4}$  ions is 1.1 nm while it is 0.6 nm for  $\text{Sn}^{+2}$ . As a result in the same ionic strength (for example in 0.1), the activity coefficient of Sn(II) is more than the activity coefficient of Sn(IV) (0.4 and 0.063 respectively) [16]. Therefore chemical potential ( $\mu$ ) as a function of molar fractions  $x_i$  and activity coefficients  $\gamma_i$  can be written as follows [14]:

$$\mu = \mu_0 + RT \sum \log x_i \gamma_i \quad (8)$$

By increasing the activity coefficient of Sn(II), its chemical potential rises. This causes the growth in the rate of chemical reaction. Thus finer grain and particle size of DPT (II) are produced due to the fact that its activity coefficient, chemical potential and rate of chemical reaction are high. According to the SEM micrographs of Fig. 2, bimodal particle size distributions could be suggested: one size around two microns and other one lower than 500 nm for both samples. The mean particle size of DPT(II) nanopowders is in the range of 0.2 to 0.7  $\mu\text{m}$  while it is 0.4 to 1  $\mu\text{m}$  for that of DPT(IV), which in turn raises the level of agglomeration. Also quantitative data from The XRD patterns confirms this result.

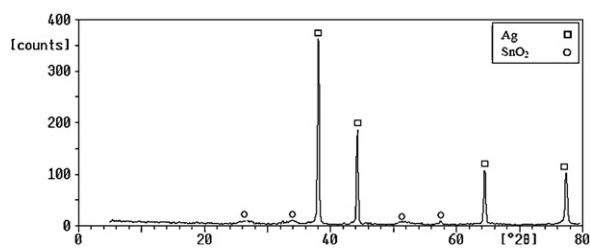


Fig. 3. X-ray diffraction analysis (XRD) patterns of DPC-I nanopowder. DPC: direct processing tin chlorine.

#### 4.2. The effect of preliminary compounds (chlorine ion)

In Fig. 1 that was recorded for DPT(II) nanopowder, the specific lines of AgCl are revealed whereas at in XRD pattern of DPC-I nanopowder in Fig. 3 it is not recognized.

The presence of some silver chloride is the result of using Sn element and HCl in the preliminary compound according to Eq. (1). SEM images of DPT(II) and DPC-I nanopowders are shown in Figs. 4 and 5. Also the X-ray mappings of both are shown in these images.

X-ray map of DPT(II) and DPC-I nanocomposites in Figs. 4 and 5 are show that Sn and Ag elements have a uniform distribution in the nanocomposites. Also Cl element has homogeneous distribution in the DPT(II) powders. According to the Fig. 1, chlorine element is present in the form of silver chloride compound. Silver chloride normally forms as a stable colloidal suspension since all of the colloidal particles are either positively or negatively charged. These charged cations or anions that are bonded to the surface of the particles [16]. Thus in the DPT(II) composite, which constitutes silver chloride particles, agglomeration occurs more than other composites.

Charged particles directly attach to the colloidal silver chloride surface, which consists of absorbed silver ions. Surrounding the charged particle is a layer of solution, called the counter-ion layer, which contains sufficient excess of negative ions to just balance the charge on the surface of the particle. The primarily absorbed silver ions and the negative counter-ion layer constitute an electric

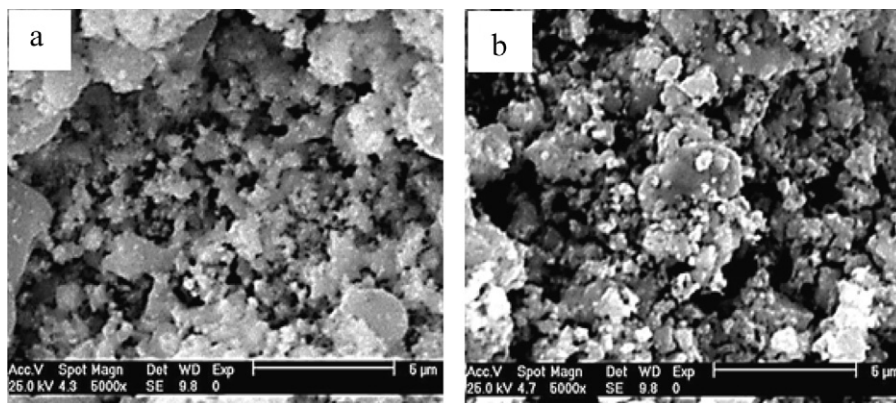


Fig. 2. Scanning electron microscopy (SEM) micrograph showing the morphology of the powders: a: DPT(II); b: DPT(IV). DPT: direct processing tin.

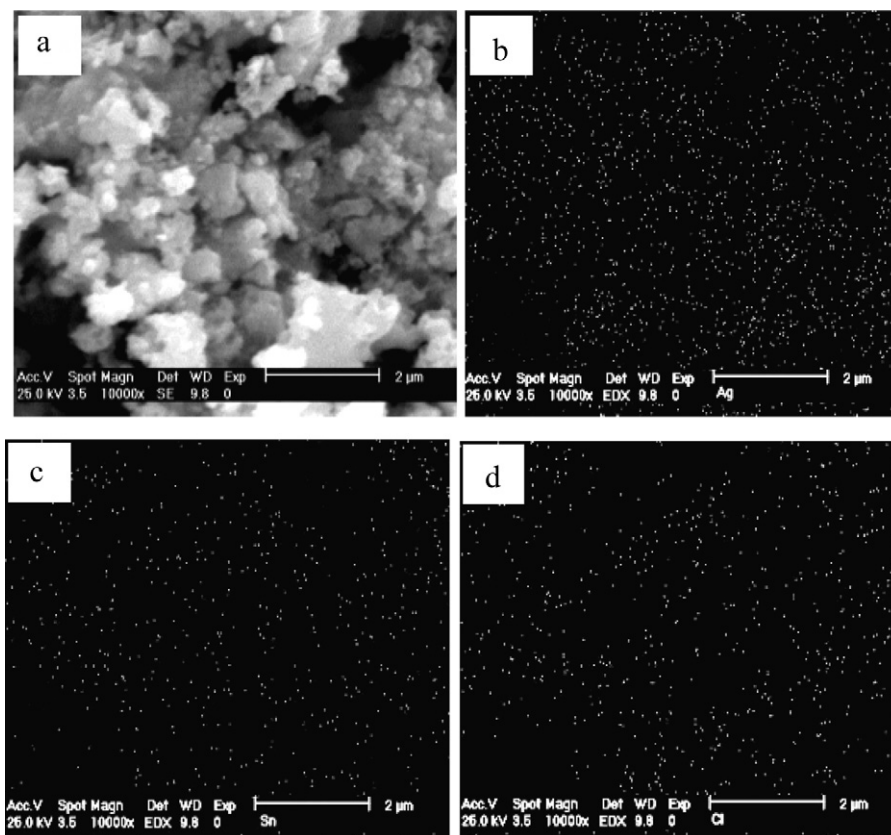


Fig. 4. The scanning electron microscopy (SEM) morphological aspects of DPT(II): a: secondary electron image; b: X-ray mapping of Ag element; c: X-ray mapping of Sn element; d: X-ray mapping of Cl element. DPT: direct processing tin.

double layer that imparts stability to the colloidal suspension. As colloidal particles approach one another, this double layer exerts an electrostatic repulsive force that prevents particles from adhering hence more growing grain and particle size [16]. So the DPT(II) powder has small size in comparison with DPC-I nanopowder. Surface tarnish films will be readily formed when exposed to chloride bearing connector environments. Silver tarnish films do not develop with a uniform morphology and can be mixed with substrate corrosion products. This can potentially lead to contact resistance issues with thinner tarnish film levels. This can make growth rate determination difficult and potentially misleading silver chloride level and contact resistance (CR) performance discrepancies between field and accelerated environment exposed silver surfaces. Silver tarnish films generally lead to CR instability at the contact interface [17]. Exposure to light slowly releases silver and chlorine (accumulation of chlorine in an enclosed space could be hazardous to person entering area). As a result chlorine ions are omitted from final component by substituting Sn by  $\text{SnCl}_2 \cdot 2\text{H}_2\text{O}$  compound.

#### 4.3. The effect of supersaturation on coprecipitation

Fig. 6 presents the morphological aspects of the DPC-I, DPC-II and DPC-III nanopowders.

The particle size of a precipitate is influenced by such experimental variables as precipitate solubility,

temperature, reactant concentrations, and rate of which reactants are mixed. The net effect of these variables can be accounted for, at least qualitatively, by assuming that the particle size is related to the relative supersaturation [16]. The supersaturation ratio ( $S$ ) is:

$$S = Q_R / K_S \quad (9)$$

In the equation, ( $Q_R$ ) is reaction quotient concept and  $K_S$  is the solubility constant. The results show that with increasing the co-precipitant concentration, crystallization and particle size decrease. A chemical precipitation process consists of three main steps: chemical reaction, nucleation, and crystal growth [15]. Nucleation occurs in the forced whirlpool region around the injection point where supersaturation is high; while the growth and agglomeration of particles can take place in the free whirlpool region far from the injection point where supersaturation is lower [18].

To obtain nanoparticles with a narrow size distribution, one should do as much as possible to meet the high degree of supersaturation. Zhou et al. used  $\text{NH}_4\text{OH}$  to precipitate cerium nitrate at room temperature [15]. They tried to obtain a high value for the supersaturation ratio ( $S$ ), in order to establish an environmental condition that favors homogeneous nucleation [16]. The crystallite size of DPC-II, obtained by X-ray line broadening technique, show that precipitation in potassium carbonate with the largest

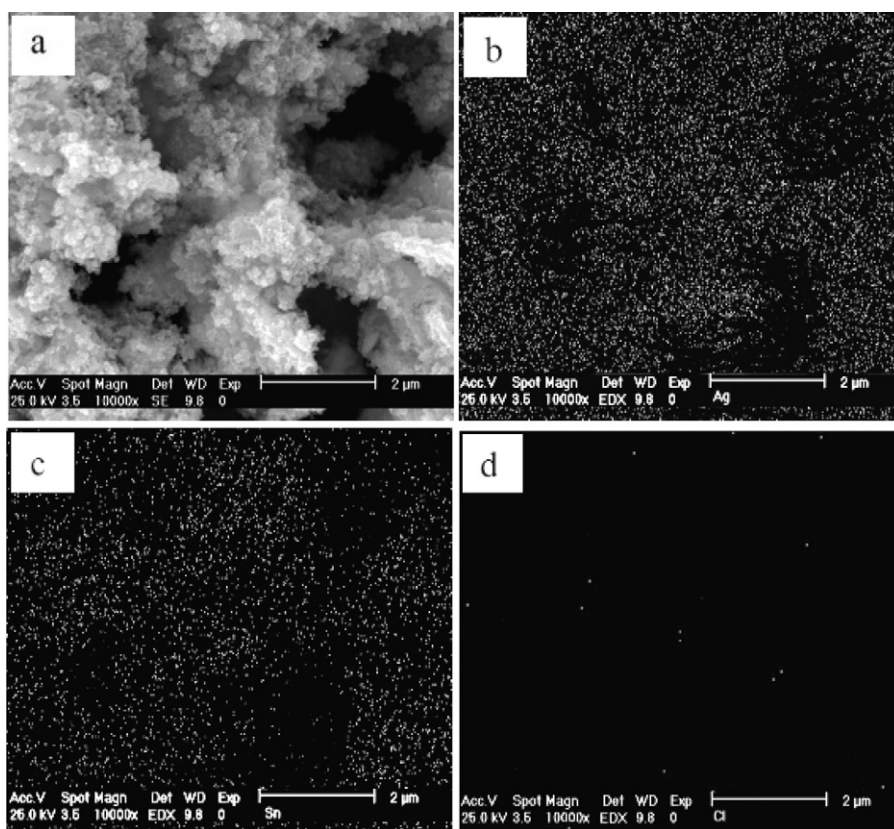


Fig. 5. The scanning electron microscopy (SEM) morphological aspects of DPC-I: a: secondary electron image; b: X-ray mapping of Ag element; c: X-ray mapping of Sn element; d: X-ray mapping of Cl element. DPC: direct processing tin chlorine.

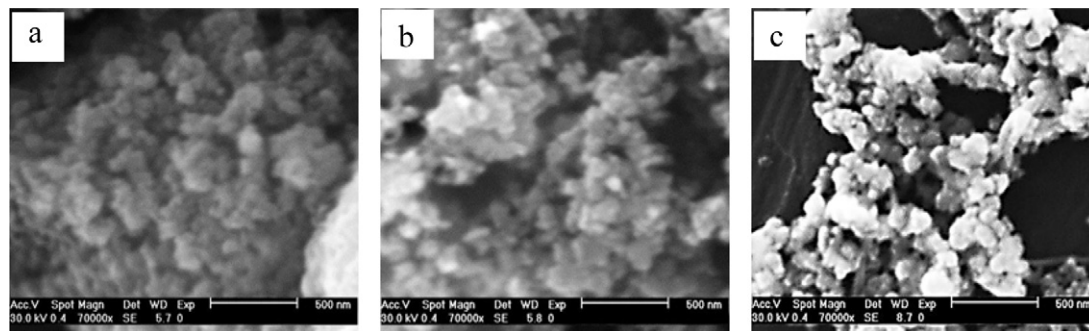


Fig. 6. The scanning electron microscopy (SEM) morphological aspects of the powders: a: DPC-I; b: DPC-II; c: DPC-III. DPC: direct processing tin chlorine.

amount of supersaturation, is smaller than other nanopowders. While the grain size of DCP-I and DCP-III, which is precipitated in sodium carbonate and sodium hydrogen carbonate with the same amount of supersaturation appropriately, are equal. In addition, SEM images of Ag-SnO<sub>2</sub> show that the particles size of DPC-II and DPC-III nanopowders in Fig. 4 are in the range of 20–60 nm and 70–120 nm, respectively. It is seen that the crystalline and particle size of nanopowders decline with the increasing of supersaturation of the precipitants.

## 5. Conclusion

Nanocomposite powder of Ag-SnO<sub>2</sub> electrical contact materials can be produced by new coprecipitation method. The oxide particles in this contact material show a uniform dispersion throughout the silver matrix. During this method, chlorine ion in the final component can be omitted by using SnCl<sub>2</sub>·2H<sub>2</sub>O in the starting materials. Also the degree of agglomeration decreases in the absence of chlorine ion. The results show increasing in the chemical

potential which happened by utilizing Sn(II) instead of Sn(IV) can help to reach lower particle and grain size. Accumulating in the supersaturation as a chemical parameter of coprecipitation method can be reduced the particle size of Ag-SnO<sub>2</sub> nanocomposite to 50%.

## References

- [1] A. Pandey, P. Verma, O.P. Pandey, *Ind. J. Eng. Mat. Sci.* 15 (2008) 229.
- [2] Y.C. Kang, S.B. Park, *Mater. Lett.* 40 (3) (1999) 129.
- [3] Verma, O.P. Pandey, A. Verma, *J. Mater. Sci. Technol.* 20 (1) (2004) 49.
- [4] P. Wu, D.Q. Yi, J. Lia, L.R. Xiao, *J. Alloys Compounds* 457 (1–2) (2008) 565.
- [5] M. Lungu, S. Gavrilu, T. Canta, M. Lucaci, E. Enescu, *J. Optoelectronics Adv.* 8 (2) (2006) 576.
- [6] J. Zheng, S. Li, F. Dou, T. Li, *Rare Met.* 28 (1) (2008) 19.
- [7] M. Rong, Q. Wang, Effects of Additives on the Ag-SnO<sub>2</sub> Contact Erosion Behavior, the Thirty-Ninth IEEE Holm Conference on Electrical Contacts, 1993, pp. 27–33.
- [8] P.B. Joshi, P. Rama krishnan, *Materials for electrical and electronic contacts, processing properties and applications*, Oxford & IBH publishing, New Delhi, 2004.
- [9] Chen, C.F. Yang, J.W. Yeh, S.S. Hung, *Metallurgic. Mater. Transac.* 36 (9) (2005) 2441.
- [10] J. Wang, M. Wen, B. Wang, J. Lu, Study on a new contact material Ag/SnO<sub>2</sub>-La<sub>2</sub>O<sub>3</sub>-Bi<sub>2</sub>O<sub>3</sub>. Proceedings of the Forty-Seventh IEEE Holm Conference on Electrical Contacts, 2001, pp. 94–97.
- [11] N. Lorrian, L. Chaffron, C. Carry, P. Deleroix, G. Lc Cacr, *Mater. Sci. Eng.* 367 (1–2) (2004) 1.
- [12] X.M. Liu, S.L. Wu, P.K. Chu, C.Y. Chung, J. Zheng, S.L. Li, *Mater. Chem. Phys.* 98 (2–3) (2006) 477.
- [13] T.Z. Yang, Z.J. Du, Preparation of Ag-SnO<sub>2</sub> composite powders by hydrothermal process, *J. Cent. South Univ. Technol.* 14 (2007) 176.
- [14] J. Wang, M. Yang, Y. Li, L. Chen, Y. Zhang, B. Ding, Synthesis of Fe-doped nanosized SnO<sub>2</sub> powders by chemical coprecipitation method, *J. Non-crystalline Solids* 351 (3) (2005) 228.
- [15] X.D. Feng, M.Z. Hu, *Encycloped. Nanosci. Nanotechnol.* 1 (1) (2004) 687.
- [16] D. Skoog, D. West, F. Holler, S. Crouch, *Fundamentals of Analytical Chemistry*, 8th edition, Brooks/Cole-Thomson Learning, USA, 2004 .
- [17] M. Myers, Overview of the Use of Silver in Connector Applications, Technical Paper, Interconnection & Process Technology Tyco Electronics, Harrisburg, PA, 2009, pp. 503–1016.
- [18] Z. Changa, D.G. Evansa, X. Duana, C. Vialc, J. Ghanbajad, V. Prevot, et al. *J. Solid State Chem.* 178 (9) (2005) 2766.